Journal of Alloys and Compounds, *176* (1991) 105–114
JAL 0002

Structural characterization of FePdP: stabilization of a new polytype of the MM'X series

M. Artigas*, M. Bacmann, D. Fruchart and P. Wolfers
Laboratoire de Cristallographie (CNRS), 166X, 38042 Grenoble Cédex (France)

R. Fruchart
Laboratoire des Matériaux et de Génie Physique UA 1109 (CNRS), ENSPG, 38402 St. Martin d'Hères (France)

(Received March 28, 1991)

Abstract

FePdP crystallizes in the space group $P\bar{6}2m$ with unit cell parameters $a = 12.055(2)$ Å and $c = 3.636(2)$ Å. It is a new type of superstructure of the Fe_2P type. However, the metal sites display different degrees of atomic disorder. The structure is analysed in terms of the phosphorus coordination polyhedra of the metal atoms, which allows it to be included among the polytypic series of MM'X (M and M', transition metals; X ≡ P, As, Si, Ge,...) phases.

1. Introduction

Most of the ternary MM'X phases (M and M', transition metals; X ≡ P, As, Si, Ge,...) belong to one of the three main structure types (Fig. 1): tetragonal T_2-Fe_2As type (space group $P4/nmm$), hexagonal H_3-Fe_2P type (space group $P\bar{6}2m$) or orthorhombic O_4-Co_2P type (space group $Pnma$). As pointed out by Fruchart [1], these structures can be built up from different packings of a pseudorhombohedral MM'X subcell (Fig. 1). This is achieved by two square-based pyramids (**P**) and two tetrahedra (**T**) formed by the phosphorus atoms. The non-metal atoms form triangular section channels running along the direction of the shortest axis of the unit cell. The channels contain alternately stacked tetrahedral and pyramidal sites, thus defining the rhombohedral subcell from two contiguous channels. The three structures are polytypes [2] when considered as 3D networks of the rhombohedral subcell.

From the above description, new types of packing can be foreseen [3]. In fact, new stackings of the rhombohedral subcell have been evidenced in $Pd_{\sim 11}Mn_{\sim 5}Ge_8$ [4] and FeRhP [5] of the NbCoB type [6].

Synthesis of ternary phosphides of composition FeMP (M ≡ Rh, Pd) presents a large number of difficulties [7]. These difficulties are connected

*On leave from the "Instituto de Ciencia de Materiales de Aragón", Zaragoza, Spain.

0925-8388/91/$3.50

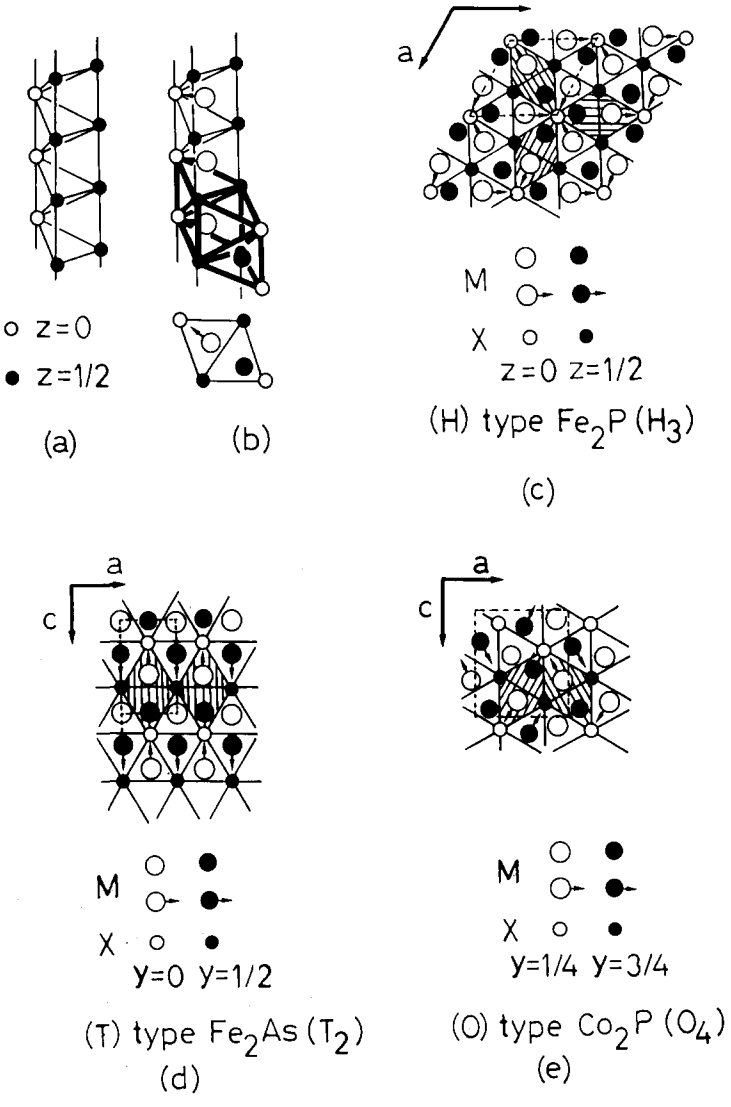

Fig. 1. (a) Triangular section channel formed by the X atoms and (b) pseudorhombohedral subcell containing two filled sites (square-based pyramid and tetrahedron) and two empty sites (square-based pyramid and tetrahedron). The three elementary packing modes of the subcells give (c) the hexagonal Fe_2P, (d) the tetragonal Fe_2As and (e) the orthorhombic Co_2P structure types.

with the successive structural transformations occurring at intermediate and high temperatures [2]. For example, FeRhP (and parent solid solutions) can be stabilized in various structures depending on the thermal treatment. Preparation of each of the polytype phases requires strict control of the synthesis parameters, otherwise the structural characterization becomes very puzzling. A polytype transformation $O_4 \Leftrightarrow H_3$ has been interpreted in terms

of cooperative displacements of phosphorus chains of half the shortest cell axis [8] and has been observed at low temperature (500 K) in both the disordered compound FeRhP and some related solid solutions [3, 9].

Among the compounds studied, the palladium-containing materials provide an opportunity to analyse the role of a nearly filled shell element on the metal ordering. Moreover, disordering effects have been observed in $(Ni_xM_{1-x})_2P$ (M ≡ Co, Ni) and MPdAs (M ≡ Ti, V, Cr) [7, 10–12].

In the present paper we report on the synthesis and structural characterization of the new phase FePdP.

2. Experimental details

2.1. Sample preparation: substitution of palladium for iron in Fe_2P

Synthesis of compounds belonging to the Fe–Pd–P system is known to be particularly ticklish because of the frequent occurrence of low melting point eutectics and the ability to form poorly crystallized and amorphous phases [13]. Powdered mixtures of FeP and palladium (1:1) annealed at various temperatures (800–1050 K) for a long time usually result in poorly crystallized specimens. Thus an alternative synthesis route was tried. Different mixtures were melted in an evacuated silica tube and subsequently quenched in order to override any possible peritectic reactions. The resulting samples were ground and then annealed at 1020 K.

We have prepared a series of intermediate compositions $Fe_{2-x}Pd_xP$. The nominal formulae of the samples studied are shown in Table 1 together with the unit cell parameters. For $x = 0.2$ the resulting compound is of Co_2P type. By increasing the palladium content to $x = 0.33$, three phases are observed to coexist: the above Co_2P type, FeP and a new phase which might be palladium richer. The broadening of the lines corresponding to the last phase is observed to be dependent on the thermal treatment, in contrast to FeP. By further increasing the palladium content, the Co_2P type phase disappears, the other two phases coexisting for $0.4 \leq x \leq 0.5$. Although the cell parameters of the FeP-type compound do not vary appreciably, those of the new phase increase with increasing palladium content. For $x = 0.8$ a few additional broad but weak lines are observed. For $x = 1$ only the new phase and very weak and diffuse signals which correspond to the additional lines ($x = 0.8$) are observed.

The new phase having almost equiatomic composition was called "FePdP" or Y (Table 1). It appears to exhibit a limited homogeneity range as indicated by the lattice parameter variations. It is clear that the system Fe_2P–FePdP does not constitute a complete solid solution: there is only a very limited range of substitutionally solid solution of palladium for iron in Fe_2P. There remains a wide range of non-solubility between the Co_2P-type and the FePdP phases. The X-ray diffraction (XRD) pattern of an as-cast sample of composition FePdP is very similar to that of a subsequently annealed and air-quenched one, but the degree of crystallization of the former remains rather poor. The

TABLE 1

$Fe_{2-x}Pd_xP$ system: unit cell parameters and volume per formula unit (V_f) for the constituent phases

x	Phase(s) present[a]	Y-type phase			Co_2P-type phase				Fe_2P-type phase		
		a (Å)	c (Å)	V_f (Å^3)	a (Å)	b (Å)	c (Å)	V_f (Å^3)	a (Å)	c (Å)	V_f (Å^3)
1.09	Y type + ?	12.0886(8)	3.6437(3)	38.427							
1.04	Y type + ?	12.0669(6)	3.6395(2)	38.246							
1	Y type + ?	12.0488(5)	3.6358(2)	38.093							
0.5	Y type + FeP	12.050(1)	3.6365(4)	38.106							
0.4	Y type + FeP	12.021(1)	3.6295(7)	37.853							
0.33	Y type + Co_2P type + FeP	12.0118(9)	3.6270(3)	37.765	5.8982(6)	3.5939(3)	6.6746(4)	35.371			
0.25	Co_2P type				5.8603(3)	3.5854(5)	6.6628(3)	34.999			
0.2	Co_2P type				5.8420(5)	3.5806(3)	6.6556(4)	34.806			
0	Fe_2P								5.8675(3)	3.4581(2)	34.367

[a]? stands for some minor unknown impurities.

corresponding XRD pattern looks like those exhibited by the M6 phase of FeRhP [3] and α-Co_2As [12]. Such a pattern can be indexed on the basis of an orthohexagonal unit cell with parameters $a \approx a_H$, $b \approx 3^{1/2}a_H$ and $c \approx c_H$ (index "H" stands for the lattice constant of an Fe_2P-type cell) or a hexagonal cell with parameters $a \approx 2a_H$ and $c \approx c_H$, with $a = 12.0488(5)$ Å and $c = 3.6358(2)$ Å. The structure should correspond to one of the three polytypes M_6, H_{12} or H'_{12} described in the crystal chemical model [2].

2.2. Powder X-ray diffraction

X-ray powder diffraction patterns have been recorded using a Guinier–Hägg camera operating with strictly monochromatized Cr $K\alpha_1$ radiation and calibrated with silicon as internal standard. From the diffraction line positions measured by using a photoscanner, the lattice parameters have been refined.

2.3. Single-crystal analysis

Some well-shaped crystals have been isolated from the melted sample corresponding to the nominal composition FePdP.

Intensity collection has been performed using an ENRAF-NONIUS CAD4 rotating anode, four-circle diffractometer controlled by a VAX/VMS computer.

The data were collected using the scan parameters reported in Table 2. The computer software package MXD [14] has been used for reduction of the data and refinement. No absorption correction was introduced owing to the small crystal size. Atomic scattering factors and anomalous dispersion corrections have been taken from *International Tables for X-ray Crystallography*.

Comparison of the formula unit volume calculated from the data with those of the parent compounds FeRhP and FeRuP [7] suggested that there were 12 formula units per cell. On the basis of the cell parameters and content, a crystal chemical model built [2] for the MM'X phases allows us to propose three hypothetical models for the structure. Only one of these, with the space group $P\bar{6}2m$, is consistent with the $6/mmm$ point symmetry (Fig. 2).

After refinement of the scale factor and the 11 position parameters, the reliability factors became stabilized at the value $R_w(F^2) = 0.261$ ($R(F^2) = 0.172$, $\chi^2 = 30.3$). Refinements of the occupancies in terms of metal atom disordering (full site occupancies) lead to $R_w(F^2) = 0.115$ ($R(F^2) = 0.106$, $\chi^2 = 5.9$). A final refinement cycle (48 variables, including the anisotropic temperature factors) yields $R_w(F^2) = 0.022$ ($R(F^2) = 0.040$, $\chi^2 = 0.95$). The final composition is $Fe_{0.966(4)}Pd_{1.034(4)}P$. The refined parameters are shown in Table 3, while Table 4 shows selected interatomic distances.

3. Description of the structure

In Fig. 2 the crystal structure of FePdP is projected on the (001) plane. All the atoms are located in planes perpendicular to the [001] direction at $z = 0$ and $\frac{1}{2}$ respectively.

TABLE 2

Data collection parameters and reliability factors

Composition	$Fe_{0.966(4)}Pd_{1.034(4)}P$
Crystal size (mm)	$0.12 \times 0.02 \times 0.03$
Space group	$P\bar{6}2m$
a (Å)	12.055(2)
c (Å)	3.636(2)
V (Å^3)	457.6
D_c (g ml^{-3})	8.4
X-ray radiation	Ag Kα
λ (Å)	0.5596
Monochromator	Graphite
Scan type/scan width (deg)	$\omega/1$
θ limits (deg)	2, 25
Standard reflections	060, 0$\bar{6}$0
No. of collected reflections	6689
No. of unique reflections	665
No. of unique reflections with $I > 3\sigma(I)$	492
Merging R	0.04
Linear absorption coefficient (cm^{-1})	110.5
Secondary extinction correction/coefficient	Le Page and Gabe/$1.93(2) \times 10^{-6}$
No. of refined parameters	48
Weights (w_i)	$2/\sigma(F_0^2)$
Reliability factors	
$R_w(F^2)$	0.022
$R(F^2)$	0.040
χ^2	0.95

The structure can be considered as a superstructure of the Fe_2P type and can be derived from the latter by $c/2$ displacements of selected phosphorus atoms (Fig. 3). This superstructure represents a new structural type in the transition metal series MM'X (X≡P, As, Si, Ge,...). According to Fruchart [1], it can be characterized by two types of blocks of rhombohedral subunits in the structural scheme of FePdP (Fig. 3): six of them form a star-shaped arrangement centred at the P(1) 1a (0, 0, 0) position, whereas the other block is composed of three rhombohedral units centred at the P(4) ($\frac{1}{3}$, $\frac{2}{3}$, 0) and ($\frac{2}{3}$, $\frac{1}{3}$, 0) atoms and projected on the (001) plane as hexagons.

In the hexagons the metal atom ordering is almost complete, iron occupying the tetrahedral (**T**) phosphorus sites and palladium occupying almost totally the pyramidal (**P**) sites. In contrast, the pyramidal site M(2) and the tetrahedral site M(1) surrounding the P(1) site exhibit disorder and contain 75.9(8)% and 65.2(7)% Pd atoms respectively. In the other metal sites of the "star-shaped block" iron only occupies the tetrahedra and palladium only occupies the pyramids.

The coordination polyhedra are those usually found in the MM'P phases [1, 15]. The phosphorus atoms are located in tetrakaidekahedra formed by the metal atoms [16].

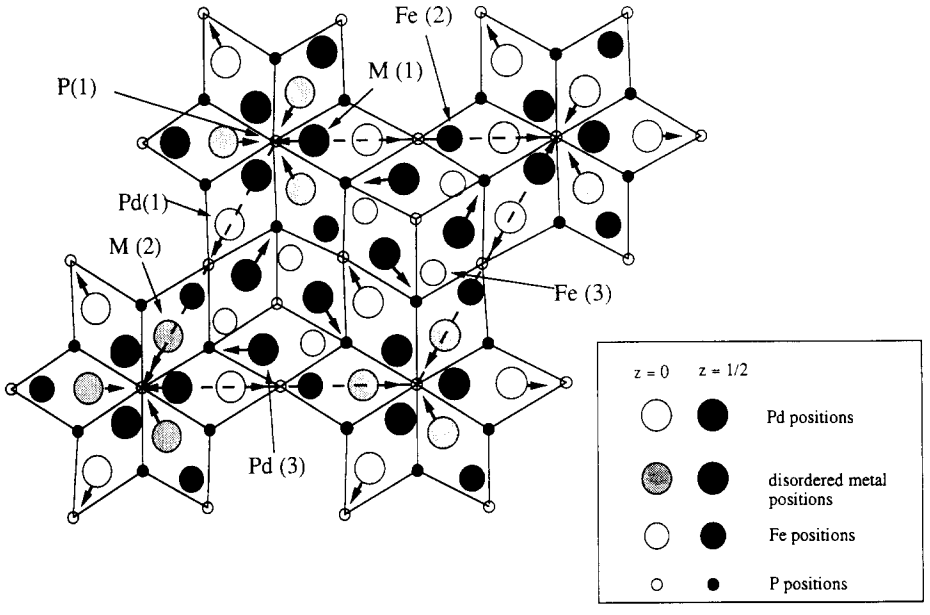

Fig. 2. Projection of the (001) plane of the crystal structure of FePdP. The numbers of the sites refer to Table 3.

TABLE 3

FePdP: positional parameters, occupancies and thermal factors[a]

Atom	Position	x	y	z	occ_{Fe}	occ_{Pd}	Angle (deg)	$\langle u_a \rangle$	$\langle u_b \rangle$	$\langle u_c \rangle$
Pd(1)	3*f*	0.32938(4)	0	0	0	1	0	99(1)	97(1)	124(1)
M(2)	3*f*	0.80279(4)	0	0	0.241(8)	1-occ_{Fe}	0	91(1)	106(1)	89(1)
Pd(3)	6*k*	0.16319(3)	0.53883(3)	0.5	0.137(3)	1-occ_{Fe}	57.0(7)	118(1)	79(1)	88(1)
M(1)	3*g*	0.14150(4)	0	0.5	0.348(7)	1-occ_{Fe}	0	96(1)	81(1)	107(1)
Fe(2)	3*g*	0.63382(7)	0	0.5	1	0	0	87(1)	78(2)	73(2)
Fe(3)	6*j*	0.18189(5)	0.72196(6)	0	1	0	92(3)	87(1)	75(1)	76(2)
P(1)	1*a*	0	0	0			0	138(3)	138(3)	120(6)
P(2)	3*f*	0.5256(1)	0	0			0	88(3)	84(3)	83(4)
P(3)	6*k*	0.34479(9)	0.1721(1)	0.5			18(4)	111(2)	91(2)	86(3)
P(4)	2*c*	1/3	2/3	0			0	83(2)	83(2)	110(3)

[a]The temperature factors are expressed as the lengths of the semiaxes of the thermal vibration ellipsoids (in 10^{-4} Å) and the angles formed by the $\langle a \rangle$ component with the crystallographic a axis (in degrees).

The metal–metal distances are larger than the corresponding sum of the 12-coordination Goldschmidt metallic radii. The metal–phosphorus distances are shorter in the tetrahedral sites and generally larger in the pyramidal ones.

We consider that there are no P–P bonds since the shortest P–P distance is 3.3 Å.

TABLE 4

FePdP: interatomic distances[a] (angstroms) shorter than 3.2 Å

		d (Å)	Σr (Å)	Δ_{ij}			d (Å)	Σr (Å)	Δ_{ij}
Pd(1)	4Pd(3)	2.9297(4)	2.74	0.07	M(1)[b]	2Pd(1)	2.9043(5)	2.70	0.09
	2M(1)	2.9043(5)	2.72	0.07		4M(2)	2.7949(4)	2.72	0.07
	2Fe(3)	2.9045(6)				2M(1)	2.9545(4)	2.70	0.04
	1P(2)	2.365(1)	2.47	−0.04		2P(3)	2.286(1)	2.45	−0.07
	4P(3)	2.691(1)	2.47	0.09		2P(1)	2.4930(3)	2.45	0.02
M(2)[b]	2Fe(3)	2.8096(8)	2.62	0.07	Fe(2)	2M(2)	2.7302(7)	2.62	0.04
	4M(1)	2.7949(4)	2.70	0.04		2Pd(3)	2.7265(8)	2.64	0.03
	2Fe(2)	2.7302(7)	2.62	0.04		4Fe(3)	2.6291(4)	2.54	0.03
	1P(1)	2.3774(5)	2.45	−0.03		2P(2)	2.2377(9)	2.37	−0.06
	4P(3)	2.664(1)	2.45	0.09		2P(3)	2.221(1)	2.37	−0.06
Pd(3)	2Pd(1)	2.9297(3)	2.64	0.07	Fe(3)	1Pd(1)	2.9045(6)	2.64	0.10
	2Fe(3)	2.7806(6)	2.64	0.05		1M(2)	2.8096(9)	2.62	0.07
	2Fe(3)	2.7283(8)	2.64	0.03		2Pd(3)	2.7806(6)	2.62	0.05
	1Fe(2)	2.7266(8)	2.64	0.03		2Pd(3)	2.7283(5)	2.64	0.03
						2Fe(2)	2.6291(4)	2.54	0.03
	2P(4)	2.5934(2)	2.47	0.05		1P(2)	2.2849(8)	2.37	−0.06
	2P(2)	2.6243(5)	2.47	0.06		2P(3)	2.256(1)	2.37	−0.05
	1P(3)	2.395(1)	2.47	−0.03		1P(2)	2.2347(8)	2.37	−0.04

[a]The values are compared ($\Delta_{ij} = 100[(-1 + d/(r_i + r_j)]$) with the sum of the Goldschmidt metallic radii for coordination number 12 and the covalent phosphorus radius for tetrahedral coordination. All distances shorter than 3.2 Å are listed. For distances involving the disordered M(1) and M(2) positions a weighted radii sum is considered.
[b]M(1) ≡ ~0.35 Fe: ~0.65 Pd; M(2) ≡ ~0.24 Fe: ~0.76 Pd.

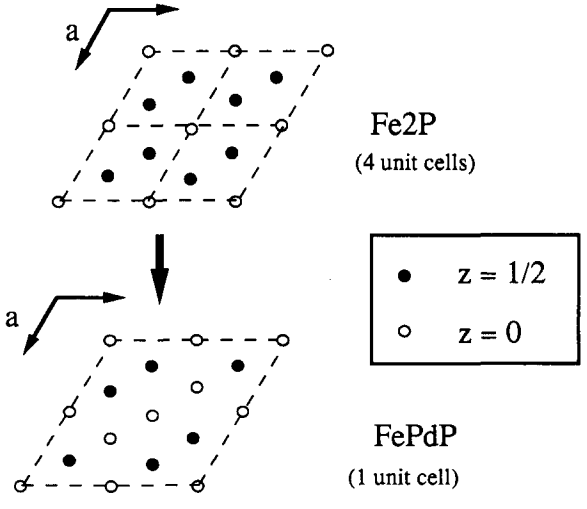

Fig. 3. The hexagonal supercell $2 \times 2H_3 \Rightarrow H_{12}$ where only phosphorus atoms are represented [3].

4. Discussion

The metal atom disordering observed on the M(1) and M(2) sites corresponds to a selective substitution effect: approximately 75% of palladium atoms in the tetrahedral M(2) position are close to the P(1) phosphorus site. Consequently, the local expansion induced by the resulting large palladium concentration around P(1) yields a weak iron substitution (about 20%) in the nearest pyramidal M(2) sites.

A systematic study of the ternaries MM'X [1, 7, 11] has indicated that the criterion of electronegativity and the criterion of atom size are two determining parameters that define the coordination of M and M' in non-metal atoms X: the atom with the highest electropositivity will be surrounded by the highest coordination number of X atoms; the atom with the largest size will choose the pyramidal site.

A study of the binary phases MM'P and MM'As, with M being a small and electropositive 3d element and M' being a bigger and less electropositive 4d element such as ruthenium, rhodium and palladium, allows us to make the above criteria competing. For M ≡ Cr, Mn the more electropositive 3d atoms occupy the pyramidal sites. In the case of M ≡ Co (smaller and less electropositive than chromium and manganese), they occupy the small tetrahedral sites. For intermediate 3d atoms such as M ≡ Fe the above factors counteract each other, which explains the total disorder found by Mössbauer spectroscopy in FeRhP and FeRhAs [7] and the partial disorder found in FeRuP [17] where the ruthenium atoms preferentially occupy the pyramidal sites.

Other specific factors have been reported such as crystal electric field effects (manganese-containing compounds [1]) and the influence of d band filling (nickel-containing compounds, *e.g.* $(Ni_xM_{1-x})_2P$ (M ≡ Fe, Co) [10, 11]).

It is note worthy that the electronegativity criterion is of little importance in FePdP. The size criterion $r_{Pd} > r_{Fe}$ well supports the almost entire filling of the smallest sites (tetrahedra) by iron. In contrast, the ordered substitution of palladium atoms on one of the two tetrahedral sites should be understood as a new ordering factor, without any connection with the non-metal polyhedron surrounding the palladium atoms.

The triangular cluster of metal atoms connecting these tetrahedra has been underlined in refs. 18 and 19 for the H_3 type (Fe_2P). At this point it appears of prime importance to emphasize the local overstoichiometry of palladium into the tetrakaidekahedron surrounding the P(1) when H_3 turns to H_{12}. One might also take into consideration that the stabilization of the new type of superstructure is related to the late 4d character of the transition element.

Acknowledgments

We wish to acknowledge Dr. A. Durif (Laboratoire de Cristallographie) for his valuable help and guidance in carrying out the intensity collection.

One of us (M.A.) is very grateful to the "Diputación General de Aragón" (Spain) for the award of a Ph.D. research fellowship number B IT-10/88. Funding from the CICYT (Spain) project MAT 88-0152 is gratefully acknowledged.

References

1 R. Fruchart, *Ann. Chim. Fr.*, *7* (1982) 563–604.
2 R. J. Angel, *Z. Kristallogr.*, *176* (1989) 193–204.
3 M. Artigas, D. Fruchart, D. Boursier and R. Fruchart, *C.R. Acad. Sci. Paris*, *310* (1990) 1621–1627.
4 G. Venturini, B. Malaman, J. Steinmetz and B. Roques, *Mater. Res. Bull.*, *16* (1981) 715–722.
5 B. Chenevier, M. Anne, P. Chaudouet, J. P. Sénateur, R. Fruchart and A. Yaouanc, *9th Int. Conf. on Solid Compounds of Transition Elements, Oxford, July 4–8, 1988.*
6 I. Krypyakevich, Yu. B. Kuz'ma, V. Voroshilov, C. B. Shoemaker and D. P. Shoemaker, *Acta Crystallogr., B 27* (1971) 257.
7 J. Roy-Montreuil, *Thèse d'Etat*, Paris, 1982.
8 B. Chenevier, J. L. Soubeyroux, M. Bacmann, D. Fruchart and R. Fruchart, *Solid State Commun.*, *64* (1987) 57.
9 M. Artigas *et al.*, to be published.
10 Y. Maeda and Y. Takashima, *J. Inorg. Nucl. Chem.*, *1* (1973) 4.
11 J. P. Sénateur, A. Rouault, P. L'Héritier, A. Krumbugel-Nylund, R. Fruchart, D. Fruchart, P. Convert and E. Roudaut, *Mater. Res. Bull.*, *8* (1973) 229.
12 A. Krumbugel-Nylund, A. Roger, J. P. Sénateur and R. Fruchart, *J. Solid State Chem.*, *4* (1977) 115.
13 G. S. Cargill, *Solid State Phys.*, *30* (1978) 227–289.
14 P. Wolfers, *J. Appl. Crystalogr.*, *23* (1990) 554–557.
15 A. Roger, *Thèse d'Etat*, Orsay, 1970.
16 S. Rundqvist, *Acta Chem. Scand.*, *14* (1960) 1961.
17 R. Wäppling, L. Häggstrom, S. Rundqvist and E. Karlsson, *J. Solid State Chem.*, *3* (1971) 276.
18 G. P. Meissner, *Ph.D. Thesis*, University of California, San Diego, 1982.
19 B. Chenevier, *Thèse d'Etat*, Grenoble, 1990.